HIROSAKI UNIVERSITY

Radiation Environment and Medicine 2023 Vol.12, No.2 99–106

REM
Radiat Environ Med

Regular Article

Effect of Off-axis Ion Recombination Factor on the Beam Profile in Flattening Filter-free Photon Beams

Yuki Tanimoto[1, 2], Masataka Oita[3]*, Shohei Yoshida[1], Atsuki Nakahira[1], Kazunobu Koshi[1] and Hirofumi Honda[4]

[1]*Department of Radiological Technology, National Hospital Organization (NHO) Shikoku Cancer Center, 160 Minamiumemotomachi, Matsuyama, Ehime 791-0280, Japan*
[2]*Graduate School of Interdisciplinary Science and Engineering in Health Systems, Okayama University, 3-1 Tsushimanaka, 3-chome, Kita-ku, Okayama, Okayama 700-8530, Japan*
[3]*Faculty of Interdisciplinary Science and Engineering in Health Systems, Okayama University, 3-1 Tsushimanaka, 3-chome, Kita-ku, Okayama, Okayama 700-8530, Japan*
[4]*Department of Radiological Technology, Ehime University Hosipital, Shitsukawa, Toon, Ehime 791-0204, Japan*

Received 19 January, 2023; revised 26 May, 2023; accepted 2 June, 2023

The ion recombination factor (k_s) of a beam without a flattening filter differs from that of a filtered beam. In this study, we examined the effect of changing the measurement conditions on k_s in the off-axis direction, and clarified the effect on the beam profile. We calculated k_s using the Jaffe plot and two-voltage method (TVM) by varying the measurement conditions, adding $k_{s,rel,\ off\text{-}ax}$ to the beam profile, and comparing the changes via local gamma analysis. The central value of k_s increased with X-ray energy, and the effect become more pronounced when the measurement depth is varied. For the beam profile with high energy and a field size of 40×40 cm^2, the results of the local gamma analysis are lower than the reference value. At the maximum dose depth, the results are poor, even when the field size is 30×30 cm^2. At 40×40 cm^2, the results are lower than the reference value even when the criteria are further relaxed. Our results indicate that k_s differs depending on the measurement method, and thus, $k_{s,rel,off\text{-}ax}$ should be considered when measuring beam profiles with field sizes larger than 30×30 cm^2.

Key words: ion recombination factor, FFF beams, beam profile, off-axis, local gamma analysis

1. Introduction

X-rays generated by a target have an intensity distribution with a sharp center[1, 2]. However, in recent years, linear accelerators that irradiate beams without flattening filters (flattening filter-free beams, FFF beams) have become popular[3].

The FFF beam can be irradiated at a higher dose rate than a beam with a flattening filter beam (WFF beam)[4], and various differences have been reported because of changes in the beam quality[5, 6]. Among them, the dose per pulse (DPP) increases and the ion collection efficiency decreases; thus, the ion recombination factor (k_s) shows a different behavior from that of WFF[7, 8].

Kry *et al*. reported that k_s measured with TN30013 changed from 1.005 to 1.008 and from 1.011 to 1.013 at a depth of 10 cm and d_{max} at 6 MV and 10 MV FFF, respectively[9]. Chang *et al*. also studied the variation of

*Masataka Oita: Faculty of Interdisciplinary Science and Engineering in Health Systems, Okayama University, 3-1 Tsushimanaka, 3-chome, Kita-ku, Okayama, Okayama 700-8530, Japan
E-mail: oita-m@cc.okayama-u.ac.jp
https://doi.org/10.51083/radiatenvironmed.12.2_99

k_s in the depth and off-axis directions and stated that by using CC13, k_s varied by 1.2% (1.015 ± 0.002 to 1.002 ± 0.001) for 6 MV FFF and by 2.0% (1.023 ± 0.006 to 1.002 ± 0.001) for 10 MV FFF[10]. Jonathan *et al*. reported that the off-axis k_s changed by up to 1.2% at 10 MV FFF when measured at intervals of 5 cm from the center in an irradiation field of 40×40 cm^2 at a depth of 5 cm using TN30013[11].

The change in k_s affects the shape of the beam profile, such as the percentage depth dose (PDD) and off-center ratio (OCR). Jonathan *et al*. reported that local gamma analysis of 40 × 40 cm^2 profiles (5 and 10 cm depths) acquired with 10 MV FFF using A1SL and CC04 with and without correction in k_s showed a gamma pass rate of 94% (>5% of the points had a gamma index greater than 1)[11].

In an FFF beam, the profile shape is convex and approximates the WFF only near the center[12]. Additionally, the convex shape varies as the irradiation field size changes; the smaller the field size, the steeper the convex shape[13].

In recent years, multiple off-axis targets have been irradiated with a single isocenter for metastatic brain tumors, and the effects of patient position rotation error and isocenter misalignment on the target dose have been investigated[14, 15]. However, the off-axis k_s that affects the OCR should not be ignored[16, 17]. Changes in the depth direction of k_s in FFF beams have been actively studied; however, studies on changes in the off-axis direction are limited. As the shape and quality of OCR vary depending on the measurement conditions, such as the size and depth of the irradiation field, previous studies are insufficient, and more detailed research is necessary.

This study had three objectives: (1) investigate the effectiveness of the two-voltage method (TVM) measurements in the off-axis direction, (2) investigate the effects of changing the measurement conditions on k_s in the off-axis direction, and (3) investigate the effect of changes in the k_s value on the shape of the beam profile, and examine whether it should be taken into account when measuring beam data.

2. Materials and methods

We used a Farmer ionization chamber (TN30013, volume 0.6 cm^3, PTW) and a small ionization chamber (Semiflex 3D, volume 0.07 cm^3, PTW), listed in Table 1. We used a RAMTEC Duo (Toyo Medic) electrometer. The target radiation was 6 MV and 10 MV X-rays (VARIAN TrueBeam STx) measured using FFF and WFF for comparison. A three-dimensional scanning water phantom, BEAMSCAN (PTW), was used. We stored the water phantom in the irradiation room at least one day before measurements to equalize with the temperature, and brought the ionization chamber into the irradiation room at least 3 h before the measurements.

To stabilize the measured values, we performed 1000 MU of pre-irradiation after applying the voltage. If the coefficient of variation (CV) exceeded 0.05%, multiple measurements were performed until the CV stabilized[18, 19].

We measured the applied voltage at five points: +100, +150, +200, +250, and +300 V because the American Association of Physicists in Medicine (AAPM) TG51 addendum recommends +300 V as the upper voltage[20].

2.1. Method for calculating the ion recombination factor

We calculated and compared the value of ion recombination factor k_s using the inverse charge (1/Q) inverse voltage (1/V) (Jaffe-plot), and TVM[21-22]. k_s can be calculated using TVM as follows.

$$k_s = a_0 + a_1\left(\frac{M_1}{M_2}\right) + a_2\left(\frac{M_1}{M_2}\right)^2 \quad (1)$$

where M_1 and M_2 are the measured values of the applied voltages V_1 and V_2, respectively, and the voltage ratio V_1/V_2 was set to 3.0 (300 V/100 V). The parameters a_0, a_1, and a_2 represent correction factors: a_0 = 1.198, a_1 = –0.875, and a_2 = 0.677.

2.2. Measurement conditions for k_s

The source-to-surface distance (SSD) was maintained at 100 cm. The ionization chamber (Semiflex 3D) was placed at a depth of 10 cm and d_{max} with field sizes of 10 × 10, 20 × 20, 30 × 30, and 40 × 40 cm^2, respectively. k_s for various depth and field sizes were measured at the center axis (CAX) as the reference value for each condition. The measurement conditions for k_s at off-axis points (i.e., distances from the CAX) were 2, 4, and 5 cm for the 10 × 10 cm^2 field; 0, 4, 8, 9, and 10 cm for the 20×20 cm^2 field; 0, 4, 8, 12, 14, and 15 cm for the 30×30 cm^2 field; and 0, 4, 8, 12, 16, 19, and 20 cm for the 40×40 cm^2 field. The measurement of each field edge (the distance from the CAX was half of each field size) was excluded at the depth of d_{max} because the chamber volume was not fully contained in the field.

First, we examined the effect of measurement depth on k_s. We measured k_s for field sizes of 10×10, 20×20, 30×30, and 40×40 cm^2, at depth of 10 cm and d_{max}, for 6 MV and 10 MV FFF. Next, to examine the changes due to the type of detector, we compared the k_s values measured using Semiflex 3D and TN30013 at depths of 10 cm and d_{max} for field sizes of 10 × 10, 20 × 20, and 30 × 30 cm^2 at 10 MV FFF. Further, to examine the difference between WFF and FFF beams, we measured and compared k_s of WFF and FFF beams at a depth of 10 cm for a field size of 30×30 cm^2 at 6 MV and 10 MV.

The shape of a beam profile changes with the measurement direction[10]. Therefore, we measured only

Table 1. Specifications of the ionization chambers

Factors	PTW Semiflex 3D 31021	PTW Farmer 300
Nominal volume (cm^3)	0.07	0.6
Length of sensitive volume (mm)	4.8	23.0
Radius of sensitive volume (mm)	2.4	3.05
Collection time (μsec)	118	140
Nominal response (nC/Gy)	2.0	0.2

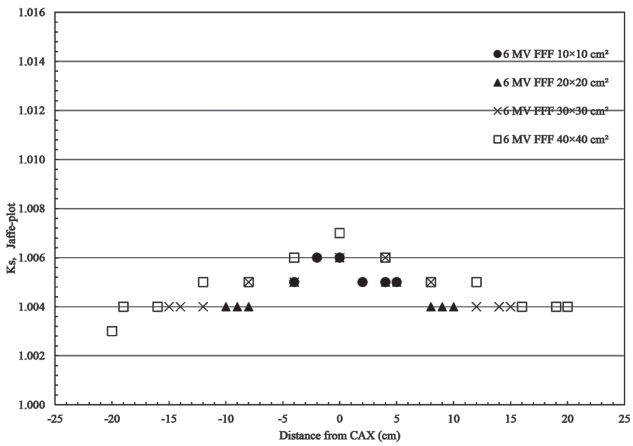

Fig. 1. k_s at each measurement point at 6 MV FFF, 10 cm depth, and field sizes of 10 × 10 , 20 × 20, 30 × 30, and 40 × 40 cm^2 (+/– direction indicates the R/L direction).

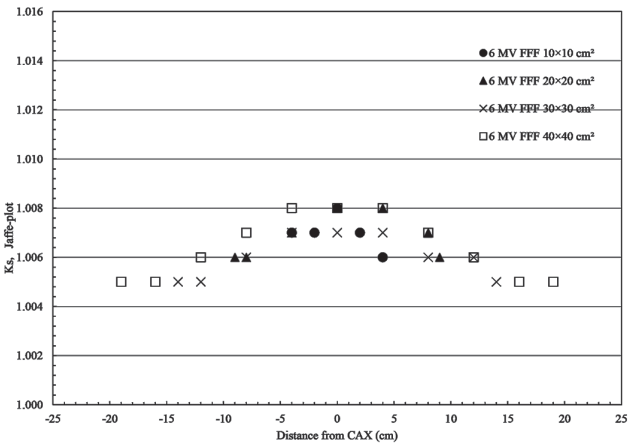

Fig. 2. k_s at each measurement point at 6 MV FFF, depth d_{max}, and field sizes of 10 × 10, 20 × 20, 30 × 30, and 40 × 40 cm^2 (+/– direction indicates the R/L direction).

for field sizes 30×30 and 40×40 cm^2 in the In-line direction at depths of 10 cm and d_{max} and compared the results with those in the Cross-line direction. To examine the effect of the change in the dose rate on k_s in the off-axis direction, we performed measurements with a 6 MV FFF beam (1400 and 400 MU/min) and 10 MV FFF beam (2400 and 400 MU/min) for a field size of 30×30 cm^2.

2.3. Calculation of relative ion recombination off-axis factors

From the obtained k_s obtained under the conditions described in section 2.2, we calculated the relative ion recombination off-axis correction factor $k_{s,rel,off\text{-}ax}$ for arbitrary points (x, y) at a depth d using Eq. (2). We set (x_0, y_0) as the beam CAX.

$$k_{s,\,rel,\,off\text{-}ax} = \frac{k_{s,}(x,\,y,\,d)}{k_{s,}(x_0,\,y_0,\,d)} \tag{2}$$

2.4. Effect on beam profile

Using Semiflex 3D, we measured the beam profile with a measurement interval of 0.5 mm, depths of 10 cm and d_{max} for field sizes 10×10, 20×20, 30×30, and 40×40 cm^2 in the Cross-line direction and 30×30 and 40×40 cm^2 in the In-line direction. We measured the energy with 6 MV FFF and 10 MV FFF and used CAX for normalization. Additionally, we performed smoothing to remove system-dependent noise in the measurement[23]. Next, for the k_s calculated under the conditions of section 2.2, we complemented the intervals between the measured points using linear interpolation and added them to the beam profile. We performed a local gamma analysis before and after the addition to calculate the gamma index to determine the effect of k_s on beam profile. The analysis was performed using the software tool, BEAMSCAN. Judgement criteria were 0.5 mm/0.5%, 0.5 mm/1%, 1 mm/1%, and 2 mm/1%, with failure defined as a gamma pass rate of less than 95%. Points outside the field were excluded because of uncertainties other than k_s.

The beam profiles were measured five times in succession under identical conditions, gamma analysis was performed for each measurement, and the average value of gamma pass rate was calculated.

3. Results

3.1. Comparison of Jaffe-plot and TVM

The Jaffe-plot and TVM results agreed within 0.1% with no tendency to overestimate or underestimate the other. In addition, no trends were observed in any of the fields, dose rates, measurement directions, or measurement points.

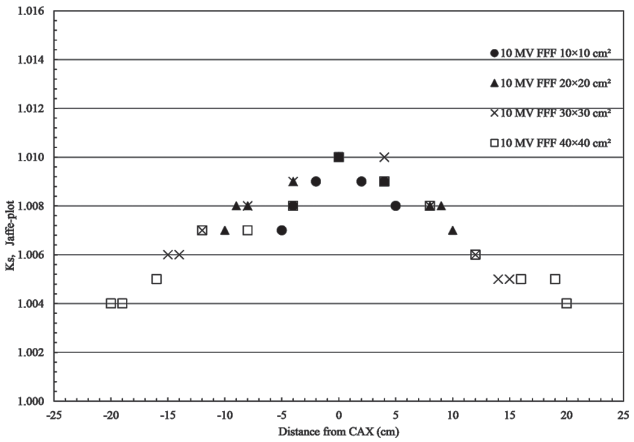

Fig. 3. k_s at each measurement point at 10 MV FFF, 10 cm depth, and field sizes of 10 × 10, 20 × 20, 30 × 30, and 40 × 40 cm^2 (+/– direction indicates the R/L direction).

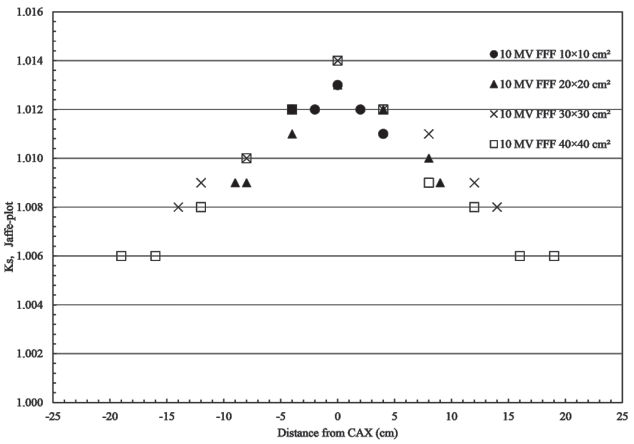

Fig. 4. k_s at each measurement point at 10 MV FFF, depth d_{max}, and field sizes of 10 × 10, 20 × 20, 30 × 30, and 40 × 40 cm^2 (+/–indicates R/L direction).

Table 2. k_s at each measurement point at a depth of 10 cm, 10 MV FFF, d_{max}, and field sizes of 10×10, 20×20, and 30×30 cm^2 due to the difference in detectors (+/– indicates the R/L direction.)

Semiflex 3D

Depth (cm)	Field size (cm^2)	Distance from CAX (cm)																		
		15	14	12	10	9	8	5	4	2	0	-2	-4	-5	-8	-9	-10	-12	-14	-15
10	10	-	-	-	-	-	-	1.008	1.009	1.009	1.010	1.009	1.008	1.007	-	-	-	-	-	-
	20	-	-	-	1.007	1.008	1.008	1.009	1.009	1.009	1.010	1.009	1.009	1.009	1.008	1.008	1.007	-	-	-
	30	1.005	1.005	1.006	1.007	1.008	1.008	1.010	1.010	1.009	1.010	1.009	1.009	1.009	1.008	1.008	1.008	1.007	1.006	1.006
d_{max}	10	-	-	-	-	-	-	-	1.011	1.012	1.013	1.012	1.012	-	-	-	-	-	-	-
	20	-	-	-	-	1.009	1.010	1.012	1.012	1.013	1.013	1.012	1.011	1.011	1.009	1.009	-	-	-	-
	30	-	1.008	1.009	1.010	1.011	1.011	1.012	1.012	1.013	1.014	1.013	1.012	1.012	1.010	1.010	1.010	1.009	1.008	-

TN30013

Depth (cm)	Field size (cm^2)	Distance from CAX (cm)																		
		15	14	12	10	9	8	5	4	2	0	-2	-4	-5	-8	-9	-10	-12	-14	-15
10	10	-	-	-	-	-	-	1.007	1.008	1.009	1.009	1.008	1.008	1.007	-	-	-	-	-	-
	20	-	-	-	1.006	1.006	1.006	1.008	1.009	1.009	1.009	1.009	1.009	1.009	1.007	1.007	1.006	-	-	-
	30	1.005	1.005	1.006	1.007	1.007	1.007	1.007	1.008	1.009	1.009	1.009	1.008	1.008	1.006	1.006	1.006	1.005	1.005	1.004
d_{max}	10	-	-	-	-	-	-	-	1.011	1.012	1.013	1.012	1.012	-	-	-	-	-	-	-
	20	-	-	-	-	1.008	1.009	1.011	1.011	1.012	1.013	10.12	1.011	1.011	1.009	1.008	-	-	-	-
	30	-	1.007	1.007	1.008	1.009	1.009	1.011	1.011	1.012	1.013	1.012	1.011	1.011	1.010	1.008	1.008	1.007	1.007	-

3.2. Variation of k_s under each measurement condition

By changing the depth from 10 cm to d_{max}, the k_s of the 6 MV FFF changed from 1.006 to 1.008 at the center (approximately 0.2%) and increased from 1.004 to 1.005 at the field edges (approximately 0.1%), as shown in Figures 1 and 2. The 10 MV FFF showed an increase of approximately 0.4% from 1.01 to 1.014 at the center, and an increase of approximately 0.2% from 1.004 to 1.006 in the limbus, as shown in Figures 3 and 4. Both the 6 MV and 10 MV FFF showed little change when compared at the same measurement point, even when the field size was changed. The edge of the field was less affected by changes in depth and energy and did not change relative to the central part.

No trend was observed when TN30013 and Semiflex 3D were compared. TN30013 had a k_s value of 1.009 at a depth of 10 cm, which changed by 0.2% at the field edge and 0.4% at the center when the depth was changed to d_{max}, as presented in Table 2.

The average value of k_s at each measurement point in the WFF was 1.004 (±0.0004) for the 6 MV WFF and 1.004 (±0.0004) for the 10 MV WFF, with little change between the center and edge of the field.

For the 6 MV FFF, the mean value of all measured points was 1.006 at the center and 1.004 at 15 cm from the center, and 1.005 (±0.0008) overall. For the 10 MV FFF, the mean value of all measured points was 1.01 at the center and 1.006 at 15 cm from the center. The mean

Table 3. k_s at each measurement point with a depth of 10 cm, 10 MV FFF, d_{max}, and field sizes of 30×30 and 40×40 cm² according to the difference in measurement direction (+/– indicates the R/L direction.)

Cross-line

Depth (cm)	Field size (cm²)	Distance from CAX (cm)																	
		20	19	16	15	14	12	8	4	0	-4	-8	-12	-14	-15	-16	-19	-20	
10	30	-	-	-	1.005	1.005	1.006	1.008	1.010	1.010	1.009	1.008	1.007	1.006	1.006	-	-	-	
	40	1.004	1.005	1.005	1.005	1.006	1.006	1.008	1.009	1.010	1.008	1.007	1.007	1.006	1.006	1.005	1.004	1.004	
d_{max}	30	-	-	-	-	1.008	1.009	1.011	1.012	1.014	1.012	1.010	1.009	1.008	-	-	-	-	
	40	-	1.006	1.006	1.007	1.007	1.008	1.009	1.012	1.014	1.012	1.010	1.008	1.007	1.007	1.006	1.006	-	

In-line

Depth (cm)	Field size (cm²)	Distance from CAX (cm)																	
		20	19	16	15	14	12	8	4	0	-4	-8	-12	-14	-15	-16	-19	-20	
10	30	-	-	-	1.005	1.005	1.006	1.007	1.009	1.010	1.008	1.007	1.006	1.005	1.005	-	-	-	
	40	1.004	1.004	1.005	1.005	1.006	1.006	1.008	1.009	1.010	1.009	1.007	1.006	1.006	1.005	1.005	1.004	1.004	
d_{max}	30	-	-	-	-	1.007	1.008	1.009	1.012	1.013	1.011	1.009	1.008	1.007	-	-	-	-	
	40	-	1.006	1.007	1.007	1.008	1.008	1.009	1.011	1.013	1.011	1.009	1.008	1.008	1.007	1.007	1.006	-	

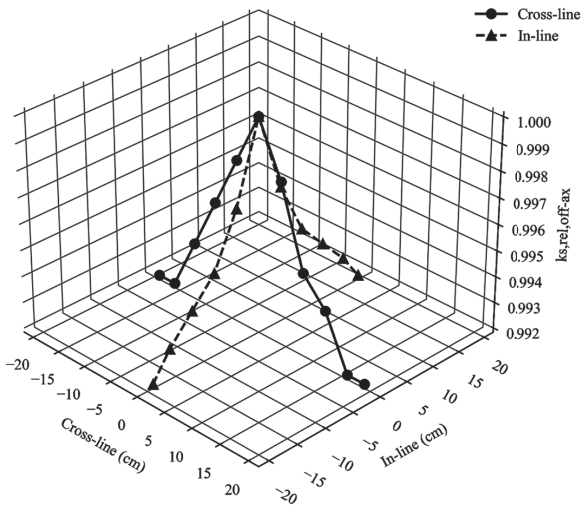

Fig. 5. $k_{s, rel, off\text{-}ax}$ in the Cross-line and In-line directions for 10 MV FFF, depth d_{max}, and irradiation field size of 40 × 40 cm² (+indicates the R and Gun directions; – indicates the L and Target directions).

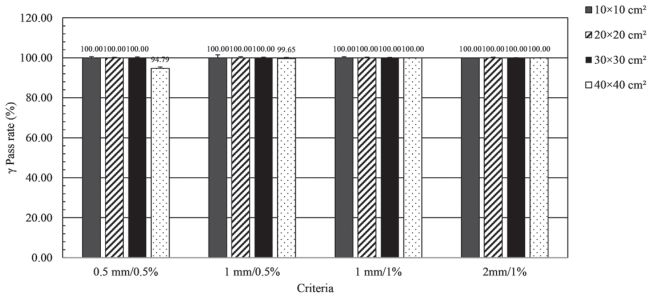

Fig. 6. Local gamma analysis in the Cross-line direction at 10 MV FFF, depth 10 cm, and field sizes of 10 × 10, 20 × 20, 30 × 30, 40 × 40 cm².

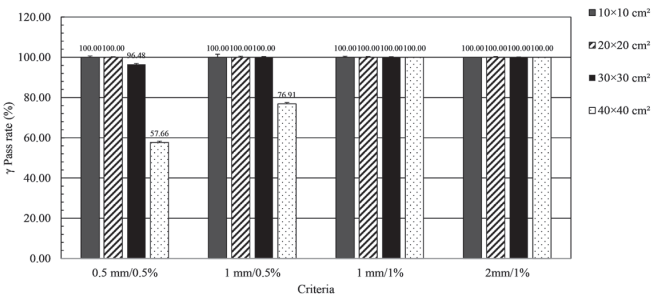

Fig. 7. Local gamma analysis in the Cross-line direction at 10 MV FFF, depth d_{max}, and field sizes of 10 × 10, 20 × 20, 30 × 30, and 40 × 40 cm².

value for all measurement points was 1.007 (±0.0018). Compared with WFF, FFF had a higher value of k_s at the center, and the convex shape is more pronounced at higher energies. As shown in Table 3, k_s varied only 0.1% at most when the measurement direction changed.

A maximum change of 0.1% was observed in both 6 MV and 10 MV FFF when the dose rate was changed. As k_s does not depend on the irradiation field size, we observed the same trend for $k_{s, rel, off\text{-}ax}$. Figure 5 shows the results of $k_{s, rel, off\text{-}ax}$ in the Cross-line and In-line directions at a 10 MV FFF, depth of d_{max}, and irradiation field size of 40×40 cm².

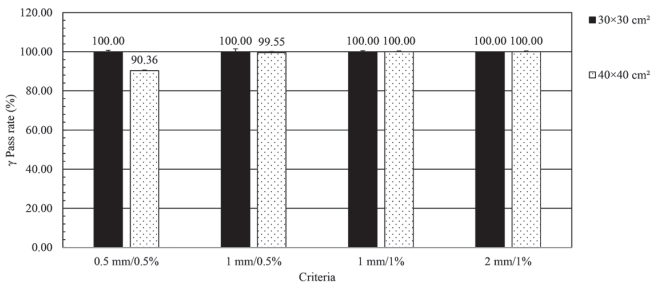

Fig. 8. Local gamma analysis in the In-line direction at 10 MV FFF, depth 10 cm, and field sizes of 30 × 30 and 40 × 40 cm².

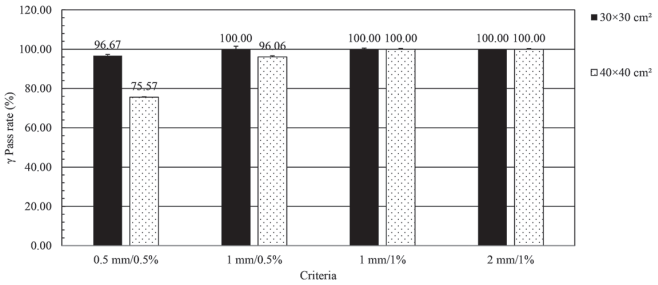

Fig. 9. Local gamma analysis in the In-line direction at 10 MV FFF, depth d_{max}, and field sizes of 30 × 30 and 40 × 40 cm^2.

3.3. Effect on Beam Profile

In the 6 MV FFF, the gamma pass rate was 100% under all conditions. In the 10 MV FFF, the pass rate was 94.79% when the depth was 10 cm with 0.5 mm/0.5% and field size 40×40 cm^2, as shown in Figure 6. At d_{max}, the change was more pronounced than that at a depth of 10 cm (76.91% at 1 mm/0.5 %), as shown in Figure 7. For a field size of 30×30 cm^2, the pass rate was 96.84%, as shown in Figure 7.

The gamma pass rates in the Cross-line direction and In-line directions were 57.66% and 75.57%, respectively, at 10 MV FFF, a field of 40×40 cm^2, and 1 mm/0.5%. As shown in Figures 7–9, the gamma pass rate significantly worsens in the Cross-line direction. The position closest to the center, where a gamma index of 1.0 or higher was counted, did not depend on the size of the field; however, d_{max} appeared closer to the center, as listed in Table 4. Toward the field edge, the uncorrected and corrected beam profiles were not aligned.

4. Discussion

The Jaffe-plot and TVM results were reported to be within 0.3% by Jonathan *et al*., which is a larger deviation than the 0.1% in our study[11]. They used an applied voltage of –250 V, which resulted in a higher k_s than the k_s in our experiments performed at +300 V. In their study, the upper limit of the applied voltage was 400 V, and the minimum applied voltage was –50 V, which caused uncertainties because of the small amount of charge.

We consider that the lack of change in k_s in the WFF beam resulted from a significant change in DPP in the FFF beam. This means that the DPP changes with depth and is higher at d_{max}. However, in the off-axis direction, the DPP did not change as much at the field edges as it did at the CAX. When correcting for k_s, understanding the change in the DPP in the off-axis direction is necessary for each profile measured at each depth.

k_s using TN30013 was 1.009 at a depth of 10 cm and 1.013 at d_{max} in the central region. These values are consistent with those reported in previous studies[9, 10].

The size of the penumbra region varied as the measurement direction changed, becoming larger in the In-line direction. The convex slope of the FFF beam depends on the field size; however, it does not affect k_s. This, together with the lack of change observed in the comparison of dose rates, confirms the results of previous studies showing that k_s depends on DPP in the off-axis direction[10].

In the analysis of beam profile, the gamma index worsened as the field size increased. Although the gamma pass rate was satisfactory (>95%), we considered performing the correction by k_s necessary when measuring fields larger than 30×30 cm^2.

Even with the worst gamma index profile, the gamma pass rate from 0.5 mm/1% was less than 95%, which is inconsistent with the results of Jonathan *et al*. who found a gamma pass rate of 94% at 40×40 cm^2 and 2 mm/1%[11]. A possible reason for the discrepancy is that the measurement interval in Jonathan *et al*. was longer (2 mm) than the 0.5 mm interval in our study, with the data interpolated between the measurement points, thereby resulting in uncertainties.

Under the conditions of 40×40 cm^2 and 1 mm/0.5%, the gamma pass rate in the Cross-line direction was much worse than that in the In-line direction. One of the possible explanations is the different CAX values. When measuring the Cross-line and In-line directions, the water phantom is often needed to be repositioned such that the

Table 4. Position closest to the center, counting gamma index 1 or more in each measurement direction, depth, field sizes of 30×30 and 40×40 cm^2, and 10 MV FFF (Cross-line: +/– indicates the R/L) (In-line: +/– indicates the Gun/Target direction).

Direction	Depth (cm)	Criteria				
		Field size (cm)	0.5 mm/0.5%		1 mm/0.5%	
Cross-line	d_{max}	30	-129.7	130.75	-	
	10	40	-169.2	194.9	-	
	d_{max}	40	-96.4	108.9	-116.5	117.9
In-line	d_{max}	30	-128.2	129.1	-	
	10	40	-169.8	167.2	-	
	d_{max}	40	-135.2	133.5	-159.1	146.5

Table 5. Gamma analysis for each measurement direction and depth for a field size of 40×40 cm² and 10 MV FFF when varying a subset of analyzed beam profiles.

Direction	Depth (cm)	Subset of profiles	Criteria	
			1.0 mm/0.5%	0.5 mm/0.5%
			Avg. gamma pass rate ± SD	Avg. gamma pass rate ± SD
Cross-line	10	All profile	0.440 ± 0.239	0.546 ± 0.301
		Outside of 15cm	0.742 ± 0.064	0.930 ± 0.070
	d_{max}	All profile	0.667 ± 0.370	0.835 ± 0.457
		Outside of 15cm	1.131 ± 0.067	1.407 ± 0.043
In-line	10	All profile	0.447 ± 0.268	0.556 ± 0.334
		Outside of 15cm	0.773 ± 0.058	0.969 ± 0.07
	d_{max}	All profile	0.561 ± 0.282	0.702 ± 0.349
		Outside of 15cm	0.904 ± 0.061	1.127 ± 0.064

short axis of the chamber faces the direction of off-axis movement. This may have caused a partial volume effect. Another possibility is that the differences in the profile shapes owing to differences in the measurement direction caused variations in the amount of charge. Furthermore, as presented in Table 5, the gamma index approaches 1.0 beyond 15 cm from CAX. As the beam profile was normalized by CAX, the slight change in the k_s value between the center and field edges may have affected the gamma pass rate at the edges. However, this variation in k_s in CAX was considered acceptable because it was equal to or less than the variation reported in the study by Chang *et al*[10].

As the value of k_s does not change when the irradiation field size changes, the same values of $k_{s,\,rel,\,off\text{-}ax}$ were added at each point. In addition, the gradient was steeper in 40×40 cm² than in 30×30 cm². Therefore, the position where the gamma index exceeds 1.0 was considered to be closer to the center. However, as presented in Table 4, the position near the center, where one or more gamma indices were counted, did not depend on the size of the field, probably because the effect of the profile slope was minimal.

The gamma index varied significantly between 1 mm/0.5% and 1 mm/1%, with the latter having no effect at all. Venselaar *et al*. reported that an accuracy of 0.5% reproducibility for deep doses is desirable. They suggested that the measurement relative depth-dose data should be 0.5%[24]. As treatment of micro-brain metastases of less than 1 cm³ was also being performed, more detailed beam data measurement was needed, and the setting of this criterion was considered appropriate[25]. Additionally, registering the beam data by adding $k_{s,\,rel,\,off\text{-}ax}$ to the profile in case of acquisition of the beam data was considered necessary. The results of this study also suggest the need for more detailed data acquisition, although the AAPM Task Group 53 reported that the accuracy of the inner beam measurement in a square irradiation field is within 1.5%[26].

A limitation of this study is that slight variations in k_s occurred when the measurement direction and irradiation field size varied. However, we were able to demonstrate the necessity of adding $k_{s,\,rel,\,off\text{-}ax}$ when measuring beam profiles. Further studies should utilize the beam data of 10 MV FFF, where the value of k_s is particularly large, and verify the influence of clinical treatment planning cases.

5. Conclusion

This study revealed that TVM can be used to measure k_s in the off-axis direction. In the FFF beam, k_s changed with the off-axis displacement from the center, and its rate of change became more pronounced when the depth changed; however, the other measurement conditions did not affect the change in k_s. We showed that $k_{s,rel,off\text{-}ax}$ must be considered when measuring profiles with a field size of 30×30 cm² or larger, and that performing measurements with strict criteria, such as 1 mm/0.5%, is necessary.

Conflict of Interest

The authors have no conflicts of interest.

Author Contribution

Yuki Tanimoto, Masataka Oita, Shohei Yoshida, Atsuki Nakahira, Kazunobu Koshi, and Hirofumi Honda designed the study. Yuki Tanimoto, Masataka Oita and Hirofumi Honda drafted the manuscript. All the authors reviewed the results and approved the final version of the manuscript.

References

1. Zelefsky MJ, Fuks Z, Happersett L, Lee HJ, Ling CC, Burman CM, *et al*. Clinical experience with intensity modulated radiation therapy (IMRT) in prostate cancer. Radiother Oncol. 2000;55(3):241–9.
2. Katsui K, Ogata T, Watanabe K, Yoshio K, Kuroda M, Hiraki T,

et al. Clinical outcome of palliative concurrent chemoradiotherapy with cisplatin/docetaxel for stage III non-small cell lung cancer. Acta Med Okayama. 2021;75(3):269–77.

3. Georg D, Knöös T, McClean B. Current status and future perspective of flattening filter free photon beams. Med Phys. 2011;38(3):1280–93.
4. Vassiliev ON, Kry SF, Chang JY, Balter PA, Titt U, Mohan R. Stereotactic radiotherapy for lung cancer using a flattening filter free Clinac. J Appl Clin Med Phys. 2009;10(1):14–21.
5. Katayose T, Kawachi T, Miyasaka R, Kodama T, Takase N, Iriyama E, *et al*. A proposal for the absorbed dose to water dosimetry for flattening filter-free beams. Jpn J Med Phys. 2016;36(2):79–84.
6. Xiong G, Rogers DWO. Relationship between %dd(10)$_x$ and stopping-power ratios for flattening filter free accelerators: a Monte Carlo study. Med Phys. 2008;35(5):2104–9.
7. Xiao Y, Kry SF, Popple R, Yorke E, Papanikolaou N, Stathakis S, *et al*. Flattening filter-free accelerators: a report from the AAPM Therapy Emerging Technology Assessment Work Group. J Appl Clin Med Phys. 2015;16(3):12–29.
8. Lang S, Hrbacek J, Leong A, Klöck S. Ion-recombination correction for different ionization chambers in high dose rate flattening-filter-free photon beams. Phys Med Biol. 2012;57(9):2819–27.
9. Kry SF, Popple R, Molineu A, Followill DS. Ion recombination correction factors (P(ion)) for Varian TrueBeam high-dose rate therapy beams. J Appl Clin Med Phys. 2012;13(6):318–25.
10. Chang Z, Wu Q, Adamson J, Ren L, Bowsher J, Yan H, *et al*. Commissioning and dosimetric characteristics of TrueBeam system: composite data of three TrueBeam machines. Med Phys. 2012;39(11):6981–7018.
11. Sutton JD, Littler JP. Accounting for the ion recombination factor in relative dosimetry of flattening filter free photon radiation. Biomed Phys Eng. 2017;3(1):017002.
12. Shimizu Y. Imadakaradekiru houshasenchiryou (in Japanese). Iryou kikigaku: The Japanese Journal of Medical Instrumentation. 2014;84(5):57–62.
13. Vassiliev ON, Titt U, Pönisch F, Kry SF, Mohan R, Gillin MT. Dosimetric properties of photon beams from a flattening filter free clinical accelerator. Phys Med Biol. 2006;51(7):1907–17.
14. Selvan KT, Padma G, Revathy MK, Raj NAN, Senthilnathan K, Babu PR. Dosimetric effect of rotational setup errors in single-isocenter volumetric-modulated arc therapy of multiple brain metastases. J Med Phys. 2019;44(2):84–90.
15. Palmiero AN, Critchfield L, Clair WS, Randall M, Pokhrel D. Single-isocenter Volumetric Modulated Arc Therapy (VMAT) radiosurgery for multiple brain metastases: potential loss of target(s) coverage due to isocenter misalignment. Cureus. 2020;12(10):e11267.
16. Clark GM, Popple RA, Young PE, Fiveash JB. Feasibitlity of single-isocenter volumetric modulated arc radiosurgery for treatment of multiple brain metastases. Int J Radiat Oncol Biol Phys. 2010;76(1):296–302.
17. Dominika JP, Klaudia MO, Krzysztof TŚ. Effects of flattening filter (FF) and flattening filter-free (FFF) beams on small-field and large-field dose distribution using the VMAT treatment plan. Pol J Med Phys Eng. 2021;27(2):137–41.
18. Hoshina M, Ogawa H, Sasamori K, Akaike H, Fukuda K, *et al*. Hysteresis phenomenon of ionization chambers for radiotherapy beams (in Japanese). Nihon Hoshasen Gijutsu Gakkai Zasshi. 2000;56(11):1348–56.
19. Shimono T. Influence on measurements of pre-irradiation due to differences in ionization chamber shape or frequency in use (in Japanese). Nihon Hoshasen Gijutsu Gakkai Zasshi. 2012;68(8):986–96.
20. McEwen M, DeWerd L, Ibbott G, Followill D, Rogers DWO, D, *et al*. Addendum to the AAPM's TG-51 protocol for clinical reference dosimetry of high-energy photon beams. Med Phys. 2014;41(4):41051.
21. Zankowski C, Podgorsak EB. Determination of saturation charge and collection efficiency for ionization chambers in continuous beams. Med. Phys. 1998;25(6):908–15.
22. IAEA. Absorbed Dose Determination in External Beam Radiotherapy: an International Code of Practice for Dosimetry Based on Standards of Absorbed Dose to Water. Technical Reports Series No. 398. Vienna: IAEA;2000.
23. Das IJ, Cheng CW, Watts RJ, Ahnesjö A, Gibbons J, Li XA, *et al*. Accelerator beam data commissioning equipment and procedures: Report of the TG-106 of the Therapy Physics Committee of the AAPM. Med Phys. 2008;35(9):4186–215.
24. Venselaar J, Welleweerd H, Mijnheer B. Tolerances for the accuracy of photon beam dose calculations of treatment planning systems. Radiother Oncol. 2001;60(2):191–201.
25. Ballangrud Å, Kuo LC, Happersett L, Boh SL, Beal K, Yamada Y, *et al*. Institutional experience with SRS VMAT planning for multiple cranial metastases. J Appl Clin Med Phys. 2018;19(2):176–83.
26. Fraass B, Doppke K, Hunt M, Kutcher G, Starkschall G, Stern R, *et al*. American Association of Physicists in Medicine Radiation Therapy Committee Task Group 53: Quality assurance for clinical radiotherapy treatment planning. Med Phys. 1998;25(10):1773–829.